

NOTES

Lys-34, Dispensable for Integrase Catalysis, Is Required for Preintegration Complex Function and Human Immunodeficiency Virus Type 1 Replication

Richard Lu, Nick Vandegraaff, Peter Cherepanov, and Alan Engelman*

Department of Cancer Immunology and AIDS, Dana-Farber Cancer Institute, and Department of Pathology, Harvard Medical School, Boston, Massachusetts 02115

Received 13 May 2005/Accepted 5 July 2005

Retroviral integrases (INs) function in the context of preintegration complexes (PICs). Two conserved Lys residues in the N-terminal domain of human immunodeficiency virus type 1 (HIV-1) IN were analyzed here for their roles in integration and virus replication. Whereas HIV-1_{K46A} grew like the wild type, HIV-1_{K34A} was dead. Yet recombinant IN_{K34A} protein functioned in *in vitro* integration assays, and Vpr-IN_{K34A} efficiently transcomplemented the infectivity defect of an IN active site mutant virus in cells. HIV-1_{K34A} was therefore similar to a number of previously characterized mutant viruses that failed to replicate despite encoding catalytically competent IN. To directly analyze mutant PIC function, a sensitive PCR-based integration assay was developed. HIV-1_{K34A} and related mutants failed to support detectable levels (<1% of wild type) of integration. We therefore concluded that mutations like K34A disrupted higher-order interactions important for PIC function/maturation compared to the innate catalytic activity of IN enzyme.

Integration is an essential step in the retroviral life cycle. It is catalyzed by the viral integrase (IN) acting upon the viral attachment (*att*) sites at the ends of linear viral cDNA within the context of a large nucleoprotein complex referred to as the preintegration complex (PIC). Soon after cDNA synthesis is completed, IN nicks specific sites at each 3' end adjacent to the phylogenetically conserved sequence CA. For human immunodeficiency virus type 1 (HIV-1), this 3' processing reaction liberates the dinucleotide pGpT from each end. Upon nuclear entry and finding a suitable target site for integration, IN joins the recessed 3' ends to the 5' phosphates of a double-stranded cut in chromosomal DNA in a coupled cleavage/ligation reaction that is referred to as DNA strand transfer. The resulting DNA recombination intermediate is flanked by single-stranded gaps that require the action of host cell DNA repair/replication enzymes to yield the integrated provirus. PICs isolated from acutely infected cells can integrate their endogenous cDNA into an added target DNA *in vitro* (4, 19, 24, 26), which yields the gapped recombination intermediate of DNA strand transfer (5, 26). IN proteins purified from a variety of sources can recombine DNA substrates that model viral *att* sites *in vitro* (7, 15, 30, 42). See reference 14 for a detailed overview of retroviral DNA integration.

IN is a three-domain protein comprised of the N-terminal domain (NTD), catalytic core domain, and C-terminal domain (CTD) as defined by results of limited proteolysis (22), functional complementation (21, 29, 41, 45), and structural biology

(12, 13, 46, 48). The NTD (HIV-1 residues 1 to 49) contains an invariant HHCC amino acid sequence motif that binds zinc (6, 8, 9, 18), and zinc binding contributes to IN multimerization and catalytic function (34, 49). It was previously determined that the substitution of Asn for His-12 (the first His in the HHCC motif) rendered HIV-1 replication defective (23), although zinc binding (8), 3' processing, and DNA strand transfer activities were reduced only a fewfold from those of wild-type IN (22). Because HIV-1_{H12N} was partially defective for the preintegration step of reverse transcription as well as postintegration particle assembly and release (23), it seemed possible that defects at steps other than integration may have contributed to the overall replication-defective phenotype of HIV-1_{H12N}. Replication-defective IN mutant viruses that display defects at steps other than integration have been labeled "class II" to distinguish them from mutants (class I) that are solely blocked at integration (20).

We recently conducted site-directed mutagenesis studies of residues conserved within the catalytic core (39) and C-terminal (37) domains of HIV-1 IN. The majority of replication-defective viruses were typed as class II mutants. Because the majority of the IN proteins derived from these mutant viruses retained catalytic function, we proposed that the viruses might be more defective for preintegration trafficking than for the catalytic steps of integration (38). In this study we targeted Lys-34 and Lys-46, two highly conserved residues within the NTD of HIV-1 IN. Whereas HIV-1_{K46A} grew as wild type, HIV-1_{K34A} was replication defective. Because the level of HIV-1_{K34A} reverse transcription was reduced five- to tenfold from that of the wild type, it was categorized as a class II mutant virus. Because recombinant IN_{K34A} protein was active in *in vitro* integration assays and Vpr-IN_{K34A} efficiently

* Corresponding author. Mailing address: Department of Cancer Immunology and AIDS, Dana-Farber Cancer Institute, 44 Binney Street, Boston, MA 02115. Phone: (617) 632-4361. Fax: (617) 632-3113. E-mail: alan_engelman@dfci.harvard.edu.

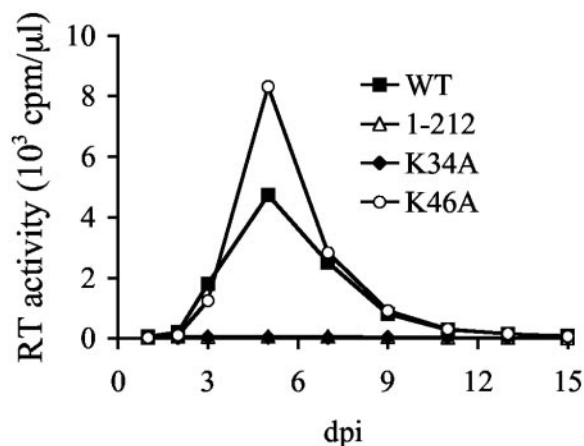


FIG. 1. Replication profiles of wild-type and mutant viruses. Cell supernatants were analyzed for RT content at the indicated times as previously described (38). Like HIV-1_{K34A}, cells infected with the negative-control CTD-deletion strain HIV-1₁₋₂₁₂ (40) failed to yield evidence of virus spread over 2 months of observation. Similar results were obtained following an independent set of infections. WT, wild type; dpi, days postinfection.

transcomplemented the infectivity defects of class I mutant viruses in cells, we concluded that HIV-1_{K34A} is another example of a replication-defective IN mutant that carries an inherently active enzyme. To directly test the integration activity of HIV-1_{K34A} PICs, as well as those derived from other class II mutant viruses, a sensitive PCR-based assay was developed to quantify in vitro DNA recombination activity. The results showed that despite containing catalytically competent IN, class II mutant PICs are devoid of DNA recombination activity.

Experimental strategy. To complete our survey of conserved residues in IN function and HIV-1 replication, Lys-34 and Lys-46 within the NTD were targeted. These solvent-accessible side chains (9, 18, 46) were highly conserved among primate lentiviral strains. Position 34 was Lys in 346 of 347 HIV-1/SIV_{cpz} strains, with Arg the sole outlier (31). Lys-46 was conserved in 345 strains, the others carrying Arg and Gln. Lys-46 was invariant among 35 additional HIV-2/SIV strains, with Arg and Lys present 30 and 5 times, respectively, at position 34 (31). To ascertain the roles of these residues in HIV-1 function, missense mutations K34A and K46A were generated in pUCWTPol (36), using QuikChange mutagenesis (Stratagene, La Jolla, Calif.). Sequence-verified 1.8-kb AgeI-PfIMI fragments were then swapped for corresponding *pol*-containing fragments in pNL43/XmaI and pNLX.Luc(R-) to generate full-length and envelope-deleted molecular clones, respectively (38).

HIV-1_{K34A} is replication defective. Titers of viral stocks made by transfecting 293T cells with full-length clones in the presence of calcium phosphate were determined using an exogenous ³²P-based assay for reverse transcriptase (RT) activity, and Jurkat T cells were infected with equal RT counts per minute of wild-type or mutant virus, as previously described (38). At the approximate multiplicity of infection of 0.04, wild-type HIV-1_{NL4-3} reached peak growth 5 days postinfection (Fig. 1). Whereas HIV-1_{K46A} also reached its peak growth at 5

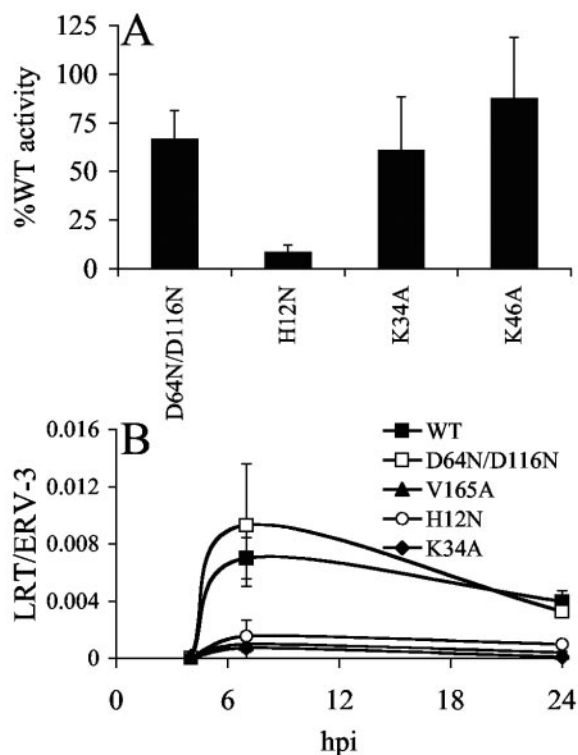


FIG. 2. Particle release and reverse transcription profiles of wild-type and mutant viruses. (A) Virus release from HeLa cells. Percentages of RT activity in relation to side-by-side transfections of wild-type HIV-1_{NL4-3}. Error bars represent results of duplicate RT assays following two independent transfections. (B) Reverse transcription profiles. Jurkat cells infected with the indicated single-round viruses were lysed at the indicated time points, and levels of HIV-1 cDNA were normalized to cellular endogenous retrovirus 3 (ERV-3), using RQ-PCR as previously described (38). Error bars are variations in results obtained from duplicate sets of RQ-PCR assays. Similar results were observed following an independent set of infections. WT, wild type; LRT, late reverse transcription.

days, HIV-1_{K34A} failed to replicate over 2 months of observation (Fig. 1 and data not shown). Thus, although similarly conserved among a large collection of primate lentiviral strains, Lys-46 was dispensable under conditions where Lys-34 played a vital role in HIV-1 replication.

Virus release and reverse transcription profiles. We next set out to characterize the detail(s) of the HIV-1_{K34A} replication block. Because a subset of replication-defective HIV-1 IN mutant viruses is defective for particle assembly/release (20), levels of viral particles in cell supernatants were quantified following transfection of HeLa cells with full-length molecular clones, using calcium-phosphate. These CD4-negative cells permitted interpretation of virus release profiles in the absence of potential viral spread. HeLa cells were also chosen for this analysis because they are more sensitive to late-stage defects than are CD4-minus 293T cells (38). The titer of HIV-1_{K34A} was similar to those of HIV-1_{K46A} and the class I mutant control strain HIV-1_{D64N/D116N} (40), indicating that viral life cycle late events were for the most part unaffected by the K34A mutation (Fig. 2A). As previously reported (23), the release of

TABLE 1. Vpr-IN complementation activities of IN mutant viruses^a

IN mutant	% WT activity ^b	Vpr-IN _{WT} ^c	% Vpr-IN _{WT} complementation ^d			
			V165A	D116A	H12N	K34A
D64N/D116N	0.2 (0.1)	19.3 (2.9)	51.4 (9.9)	0.4 (0.1)	2.2 (1.7)	26.5 (8.1)
V165A	0.1 (0.1)	56.1 (17.8)	0.3 (0.1)	3.2 (0.6)	0.1 (0.0)	5.0 (0.9)
H12N	0.1 (0.0)	60.8 (23.6)	0.3 (0.1)	0.3 (0.1)	0.1 (0.1)	1.2 (0.3)
K34A	0.1 (0.1)	33.3 (14.3)	2.2 (0.5)	1.7 (1.0)	0.2 (0.1)	4.3 (2.5)
W235E	0.2 (0.1)	40.6 (22.4)	4.6 (1.5)	8.9 (2.4)	1.3 (0.2)	36.8 (18.1)

^a Average of duplicate luciferase activities following two independent infections, with standard deviation in parentheses.

^b Mutant virus activity relative to that of HIV-1_{NLX.Luc(R-)}. WT, wild type.

^c Vpr-IN_{WT} complementation activity relative to that of HIV-1_{NLX.Luc(R-)}.

^d Activity of the indicated Vpr-IN mutant protein, relative to that of Vpr-IN_{WT}.

the NTD mutant HIV-1_{H12N} was significantly reduced from that of the wild type (Fig. 2A).

Numerous mutations in HIV-1 IN alter reverse transcription (20). To facilitate this analysis, single-round derivatives of wild-type and mutant viruses were utilized to restrict the potential for virus spread during infection of CD4-positive cells. The titers of transcomplemented viruses made by cotransfecting 293T cells in the presence of FuGENE 6 (Roche Molecular Biochemicals, Indianapolis, Ind.) with envelope-deleted molecular clones and the HIV-1_{NL4-3} envelope expression vector pNLXE7 were determined, and the viruses were treated with 40 U TURBO DNase (Ambion, Austin, Tx.)/ml for 1 h at 37°C as previously described (39). Jurkat T cells infected with equal RT counts per minute of wild-type or mutant virus via spin-oculation were lysed, using a DNeasy kit (QIAGEN, Valencia, Calif.), and levels of late reverse transcription products were determined, using real-time quantitative (RQ)-PCR as previously described (39). HIV-1 levels were normalized to the cellular marker endogenous retrovirus 3, and signals detected in parallel infections with wild-type or mutant viral supernatants lacking envelopes were subtracted from envelope-mediated infections to correct for input plasmid DNA that may have resisted DNase digestion (39).

HIV-1_{NLX.Luc(R-)} cDNA synthesis was below the limit of detection at 4 h postinfection (hpi) and peaked at approximately 7 hpi (Fig. 2B). Consistent with previous reports (39, 40), reverse transcription of class I mutant HIV-1_{D64N/D116N.Luc(R-)} was similar to that of the wild-type virus at 7 hpi (Fig. 2B). In sharp contrast, HIV-1_{K34A.Luc(R-)} cDNA levels were reduced approximately tenfold from that of the wild type at 7 hpi (Fig. 2B). This reduction was similar to the partial reverse transcription defects displayed by previously described class II mutants HIV-1_{H12N.Luc(R-)} (23) and HIV-1_{V165A.Luc(R-)} (38) (Fig. 2B). Because levels of class II mutant viral reverse transcription remained low at 24 hpi, we concluded that the reductions observed at 7 hpi were due to overall impairment of cDNA synthesis capacity rather than slow kinetics of reverse transcription (Fig. 2B) (39).

A minor fraction of retroviral cDNA is ligated via host-mediated nonhomologous DNA end joining in cell nuclei to yield circles with two adjoining copies of the viral long terminal repeat (LTR) (reference 35 and references therein). The fraction of HIV-1_{K34A.Luc(R-)} cDNA present as 2-LTR circles at 24 hpi was similar to the wild-type fraction, indicating that the mutation did not impair PIC nuclear localization (data not shown).

IN_{K34A} can catalyze HIV-1 integration. Because the level of HIV-1_{K34A.Luc(R-)} reverse transcription was similar to that of previously characterized class II mutant strains (Fig. 2B), HIV-1_{K34A} was categorized as a class II IN mutant virus. The IN proteins derived from certain class II mutant viruses were catalytically active despite crippling blocks to viral preintegration function (38). In these cases, catalysis was demonstrated using purified recombinant proteins in *in vitro* integration assays and phenotypic complementation by Vpr-IN during HIV-1 infection. The infectivity defect of IN mutant viruses can be restored by transpackaging wild-type IN as a Vpr-IN fusion protein during HIV-1 assembly (25, 47). In addition, we and others have shown that fusion proteins derived from certain class II IN mutant viruses efficiently transcomplemented the infectivity defects of class I active site mutant reporter strains (1, 25, 38, 39, 43). To test the catalytic potential of IN_{K34A} in the context of virus infection, the K34A mutation was introduced into the pRL2P-Vpr-IN expression vector (obtained from J. Kappes, University of Alabama) as previously described (38). Single-round reporter viruses carrying the gene for firefly luciferase with or without added Vpr-IN were generated by cotransfecting 293T cells as previously described (38). Two previously characterized class I mutant viruses, HIV-1_{D64N/D116N.Luc(R-)} (38) and HIV-1_{W235E.Luc(R-)} (32, 37), as well as two class II mutant viruses, HIV-1_{H12N.Luc(R-)} (23) and HIV-1_{V165A.Luc(R-)} (38), served as controls. Jurkat T cells infected with equal RT counts per minute of reporter viral supernatants were processed for luciferase assays as previously described (38). Luciferase activities were normalized to total cell protein as determined by the Bio-Rad protein assay kit (Bio-Rad Laboratories, Hercules, Calif.).

As previously established (1, 38), the Vpr-IN_{V165A} fusion protein efficiently transcomplemented the infectivity defect of class I mutant HIV-1_{D64N/D116N.Luc(R-)} (Table 1). In contrast, Vpr-IN_{V165A} failed to restore significant function to either class II mutant control strain. Vpr-IN_{V165A} restored approximately 2% of Vpr-wild-type IN (IN_{WT}) function to HIV-1_{K34A.Luc(R-)} (Table 1), which is consistent with previous observations that class II mutant viral INs tend to poorly transcomplement the infectivity defects of class II mutant reporter viruses (38).

Because Vpr-IN_{K34A} transcomplemented the infectivity defect of HIV-1_{D64N/D116N.Luc(R-)} at approximately 27% of the level of Vpr-IN_{WT}, we concluded that IN_{K34A} could integrate HIV-1 cDNA during virus infection. Vpr-IN_{K34A} also effi-

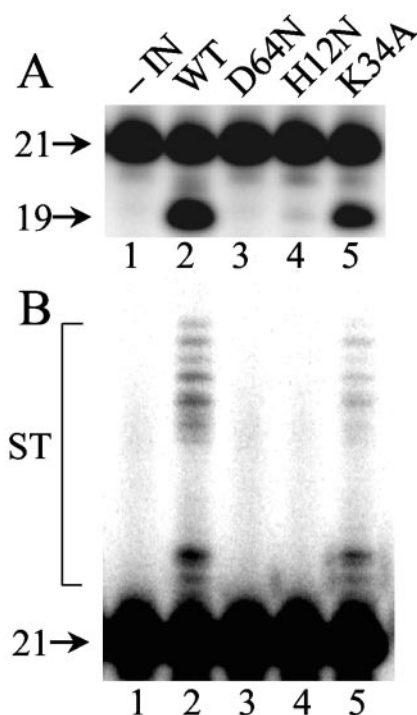


FIG. 3. Wild-type and mutant IN activities. (A) 3' Processing activity. Aliquots of integration assays conducted as previously described (38) were analyzed on polyacrylamide sequencing gels. 21, migration position of substrate DNA; 19, migration position of the 3' processing reaction product. (B) Longer autoradiographic exposures revealed products of DNA strand transfer (ST) in lanes 2 and 5. IN was omitted from the reaction in lanes 1. Results are representative of those obtained in two independent assays. WT, wild type.

ciently complemented at least one other class I mutant virus, HIV-1_{W235E.Luc(R-)} (Table 1). Because Vpr-IN_{H12N} inefficiently complemented class I mutant virus function, we concluded that IN_{H12N} was for the most part inactive under these assay conditions (Table 1).

The results of Vpr-IN complementation demonstrated that IN_{K34A} could function in concert with IN_{D64N/D116N} or IN_{W235E} to integrate HIV-1 cDNA *in vivo*. To address the catalytic potential of IN_{K34A} in the absence of a second mutant IN protomer, the mutation was introduced into the bacterial expression vector pKBIN6H, and recombinant His₆-tagged IN purified from soluble extracts of *Escherichia coli* cells was reacted with a 21-bp oligonucleotide modeling the U5 *att* site as previously described (38). Wild-type IN converted approximately 34% of the substrate to the nicked 3' processing product following 1 h at 37°C (Fig. 3A, lane 2). Because IN_{K34A} displayed about 50% of the level of wild-type activity (Fig. 3A, compare lane 5 to lane 2), we concluded that it is an active enzyme. Longer exposure of the autoradiogram demonstrated that IN_{K34A} supported DNA strand transfer activity at a level that was proportional to its 3' processing activity (Fig. 3B). IN_{H12N}, in contrast, supported only about 1% of wild-type IN function (Fig. 3A, lane 4).

A novel, sensitive RQ-PCR assay for HIV-1 PIC function. Because numerous class II IN mutant proteins efficiently functioned in Vpr-IN transcomplementation and *in vitro* integra-

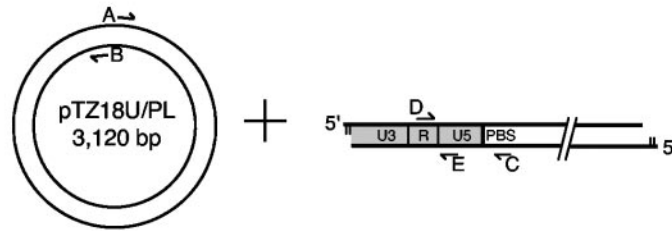
tion assays, an outstanding issue was whether the PICs derived from the corresponding replication-defective mutant viruses catalyzed integration (38). Using Southern blotting, we previously failed to detect HIV-1_{V165A} PIC activity *in vitro* (36). Considering that many class II IN mutations significantly impair reverse transcription, the detection of mutant PIC activity by Southern blotting can have its limitations, and because of this, we developed a novel PCR-based assay to quantify levels of HIV-1 PIC activity in *in vitro* integration assays. Although two groups previously reported RQ-PCR assays for PIC function (2, 27), we felt each of these had its limitations in terms of ease of setup and routine performance. Whereas the assay described by Hansen and colleagues (27) required the covalent attachment of sheared target DNA to plate wells, Brooun et al. utilized a linearized 3.4-kb restriction fragment containing 32 repeats of a 105-base unit as the target and, due to the relatively large number of repeats, integration reactions were treated with λ exonuclease prior to deproteinization and PCR (2). To simplify, we designed an assay utilizing circular plasmid DNA as the target. Whereas Southern blotting can distinguish the integration of a single viral cDNA end from the concerted integration of both *att* sites that are normally catalyzed by HIV-1 PICs (10), the following assay quantifies the integration of the U3 DNA end. We note that the previous RQ-PCR assays for PIC function likewise monitored integration of just one HIV-1 end (2, 27).

The assay is outlined in Fig. 4. Five different PCR primers, A to E, were designed (Fig. 4A). Primers A (AE2413; 5'-GT TGTTCAGTTTGGAAACAAGAGTC) and B (AE2414; 5'-A CTCAACCCTATCTCGGTCTATTC) annealed to opposite strands of the plasmid. Primer C (AE2257; 5'-TTTCAGGTC CCTGTTCGGCGCCAC) annealed to the plus strand of the HIV-1 primer binding site (HIV-1_{NL4-3} nucleotides 665 to 635), and primers D (AE1068; 5'-GGTCTCTCTGGTTAGACCAG; HIV-1_{NL4-3} nucleotides 455 to 474) and E (AE1069; 5'-GATCTCTAGTTACCAGAGTC; HIV-1_{NL4-3} nucleotides 596 to 577) annealed to the minus and plus strands within the R and U5 regions of the LTR, respectively.

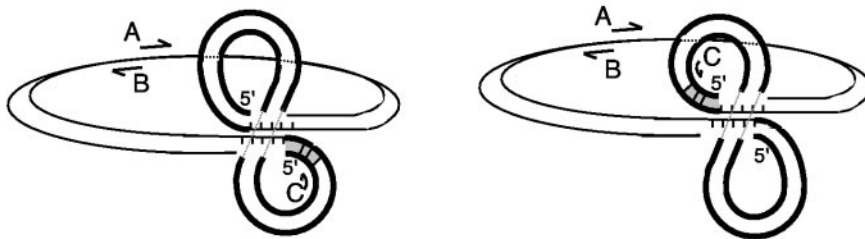
The assay detects upstream LTR (Fig. 4A and B, gray box)-target DNA junctions that form during integration. The upstream LTR will join to either strand of the plasmid, and employing primers that annealed to both strands of target DNA gave the opportunity to detect most if not all integration events (Fig. 4B). To increase the sensitivity of detection as well as to quantify assay readout, the products of first-round amplification were diluted into RQ-PCR assays, which were developed using nested HIV-1 primers D and E (Fig. 4C).

HIV-1_{IIIIB} PICs were isolated from cocultures of chronically infected MOLTIIB cells and uninfected CD4-positive SupT1 cells as previously described (11). RNase A-treated (20 μ g/ml for 30 min at room temperature) cytoplasmic extract (350 μ l) was either placed on ice (Fig. 5A, -target) or adjusted to contain 8 mM EDTA (Fig. 5A, +EDTA), 10 μ M IN inhibitor L-731,988 (28) (Fig. 5A, +L-731,988), or 0.005% (vol/vol) dimethyl sulfoxide (DMSO) (Fig. 5A, +target) to match the amount of DMSO introduced by the inhibitor. Plasmid DNA was added to the final concentration of 3 μ g/ml to the EDTA-, drug-, and DMSO-treated samples, and integration proceeded for 45 min at 37°C. Following deproteinization and precipitation with ethanol, samples were resuspended in 50 μ l of TE.1

A. Primer design



B. *In vitro* integration products



C. First-round and nested PCR products

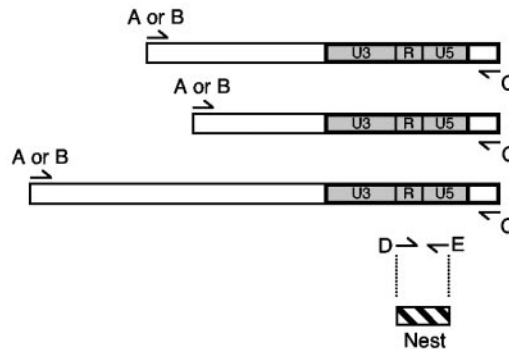


FIG. 4. Design of a novel PIC integration assay. (A) Locations of PCR primers. Plasmid pTZ18U/PL (16) (thin lines) was obtained from H. Göttlinger (University of Massachusetts Medical School). The upstream LTR (bold lines, viral cDNA) is shaded gray. See text for details of primer sequences/locations. (B) *In vitro* integration products. The U3 end of the upstream LTR will integrate into either strand of pTZ18U/PL. (C) PCR products. One terminus of all first-round products is defined by primer C, and the other end contains sequences defined by primer A or B. The amount of nested product amplified using primers D and E (hatched box) was quantified using RQ-PCR. PBS, primer binding site.

buffer (10 mM Tris-HCl [pH 8], 0.1 mM EDTA). Because EDTA (4, 24) and L-731,988 (28) inhibited PIC function, only the +target sample was expected to yield integration products.

The first-round PCR (50 μ l) contained 5 μ l of the sample, 0.5 μ M each of primers A, B, and C, 200 μ M each deoxynucleoside triphosphate, and 1.25 U of HotStarTaq DNA polymerase in buffer supplied by the manufacturer (QIAGEN). Following an initial incubation at 95°C for 15 min, reactions proceeded through 18 cycles of denaturation (94°C for 30 s), annealing (58°C for 30 s), and extension (72°C for 4 min) before a final 10-min extension at 72°C. First-round products were diluted 1:1,000 with H₂O, and 5 μ l was analyzed in duplicate by RQ-PCR (30 μ l), using a QuantiTect SYBR Green PCR kit (QIAGEN) and 0.3 μ M each of primers D and

E. After an initial incubation at 95°C for 15 min, reactions were cycled 40 times through 15 s of denaturation at 94°C, 30 s of annealing at 58°C, and 30 s of extension at 72°C, using a DNA Engine Opticon thermal cycler (MJ Research Inc., Waltham, Mass.). Results were analyzed using OpticonMONITOR Analysis software, version 2.01, supplied by the manufacturer. Melting curve analyses revealed a tightly bunched population of profiles whose average strand dissociation temperature was approximately 81°C, indicating that a single, specific DNA species was amplified by RQ-PCR (data not shown).

To determine the linearity of the assay, the +target sample was serially diluted (fourfold steps) to a final concentration of 1:4,096 prior to first-round amplification. The response fit well to ideal linear behavior, generating a standard curve with $r^2 =$

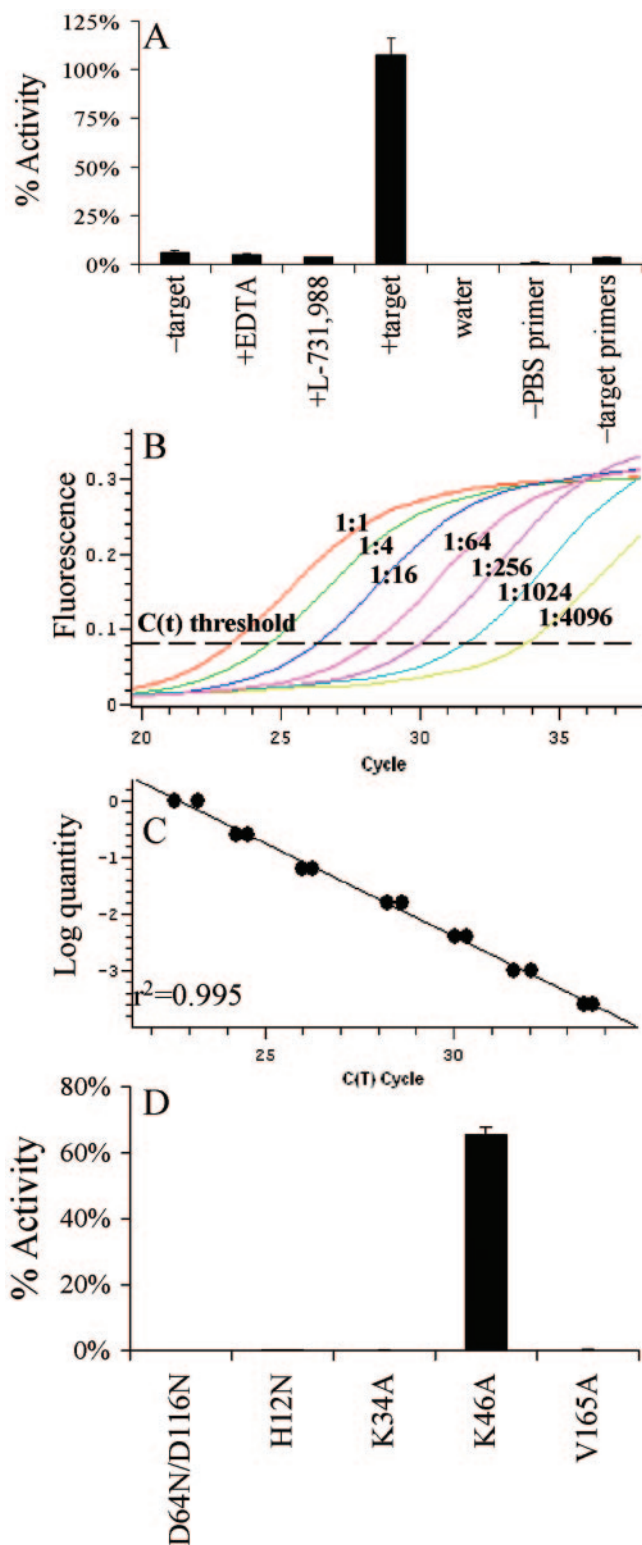


FIG. 5. Results of in vitro PIC assays. (A) HIV-1_{IIIIB} PIC activity levels under various experimental conditions. See text for details. Error bars represent the variation in results observed between duplicate RQ-PCR assays. water, activity obtained (0.13%) from using water in the first-round PCR. (B) Amplification curves of various dilutions of the +target sample (see text). Cycle threshold [C(t)] was set to maximize the r^2 value of the corresponding standard curve. Although samples were run in duplicate, only one example of each dilution was

0.995 (Fig. 5B and C). Comparing the cycle threshold values of the -target, +EDTA, and +L-731,988 samples to the standard curve revealed relative integration activities of approximately 5.9%, 4.8%, and 3.7%, respectively (Fig. 5A). Because the -target sample lacked plasmid DNA, we reasoned that these apparent activity levels were likely due to residual levels of unintegrated HIV-1 cDNA introduced into second-round PCRs upon dilution. To address this, the +target sample was reanalyzed, omitting from the first round either primer C (Fig. 5A, -PBS primer) or primers A and B (Fig. 5A, -target primers). Whereas the -PBS primer sample yielded approximately 0.8% activity, the -target primer sample revealed about 3.2% activity (Fig. 5A). This indicated that the low levels of activity detected in the absence of target DNA or in the presence of EDTA or L-731,988 were mainly due to first-round asymmetric amplification of HIV-1 cDNA via primer C. We concluded that the assay was linear, yielding an approximate 20- to 30-fold response over unreacted HIV-1 cDNA (Fig. 5A to C).

Class II IN mutant viruses yield defective PICs. In vitro integration activities of wild-type and IN mutant PICs were analyzed next. Virus supernatants (20 ml) from 293T cells transfected with full-length molecular clones using FuGENE 6 were treated with TURBO DNase as described above. RNase A-treated cytoplasmic extracts (2 ml) isolated from C8166 T cells (3×10^7) at 7 hpi (11) were split into two samples (0.9 ml), pTZ18U/PL was added to one, and integration proceeded as described above. Deproteinized and precipitated DNAs were resuspended in 40 μ l of TE.1.

Because class II mutant viruses were partially defective for reverse transcription (Fig. 2B) (20, 37–39), it was important to normalize in vitro PIC activities to the different viral cDNA levels that formed during infection. For this, -target samples (5 μ l) were analyzed in duplicate by RQ-PCR using the QuantiTect SYBR Green PCR kit and 0.3 μ M each of gag-specific primers AE1070 (5'-GAAGCTGCAGAATGGGATAG; HIV-1_{NL4-3} nucleotides 1411 to 1430) and AE1071 (5'-GGTACTAGTAGTTCCTGCTA; HIV-1_{NL4-3} nucleotides 1515 to 1496). Reactions cycled as before were normalized to a standard curve created by fivefold dilutions (from 25,000 to 20 copies) of pNL43/XmaI (3). HIV-1_{D64N/D116N} yielded approximately 110% of the level of wild-type HIV-1_{NL4-3} cDNA, HIV-1_{H12N} about 10% of that of the wild type, HIV-1_{K34A} about 21% of that of the wild type, HIV-1_{K64A} about 62% of that of the wild type, and HIV-1_{V165A} about 26% of that of the wild type. Minus-target and +target samples were analyzed for in vitro PIC activity, and the resulting -target values, which ranged from 0.04% to 1.0% of wild type integration activity, were subtracted from corresponding +target values. Levels of in vitro PIC activities were then normalized to total cDNA levels.

As expected (11), the class I active site mutant HIV-1_{D64N/D116N} failed to support appreciable levels of in vitro PIC

shown for clarity. (C) Duplicate results from panel B plotted as log quantity response versus C(t) cycle number. This defined the standard curve utilized in panel A. (D) Wild-type and mutant HIV-1_{NL4-3} PIC activity levels. Levels were expressed as percentages of wild-type activity. Error bars indicate the variations in results obtained between duplicate RQ-PCR assays.

activity (<0.5% of wild-type activity; Fig. 5D). Class II mutants HIV-1_{H12N}, HIV-1_{K34A}, and HIV-1_{V165A} displayed similar low levels of activity (0.5% to 0.75% of that of wild type; Fig. 5D). In contrast, replication-competent HIV-1_{K64A} supported about 66% of wild-type PIC activity. This analysis confirmed our previous results with HIV-1_{V165A} PICs (36) and extended them to include HIV-1_{K34A}, a separate class II mutant virus whose IN efficiently functioned in in vitro integration (Fig. 3) and Vpr-IN complementation (Table 1) assays. Our results also established an in vitro PCR-based PIC integration assay that, after correction for unintegrated HIV-1 cDNA levels, afforded approximately two orders of magnitude of sensitivity (Fig. 5).

IN enzyme function and HIV-1 replication. Through employing a novel, sensitive PCR-based assay for PIC function (Fig. 4), we determined that PICs derived from class II mutant viruses like HIV-1_{V165A} and HIV-1_{K34A} failed to support detectable levels of in vitro integration activity (Fig. 5), despite the fact that the mutant IN proteins were catalytically active in in vitro integration assays and in cell-based Vpr-IN complementation assays (Table 1; Fig. 3) (1, 38). We noted that this phenotype is not restricted to class II IN mutations. The W235E CTD mutation yielded the class I replication-defective phenotype (32), although IN_{W235E} supported wild-type levels of in vitro integration activities (33) and Vpr-IN_{W235E} efficiently transcomplemented HIV-1_{D64N/D116N.Luc(R-)} function (37). Akin to the results reported here, we previously determined that HIV-1_{W235E} PICs failed to support detectable levels of in vitro integration activity (11).

Based on results of Vpr-IN complementation, the mutant IN proteins can function in the context of HIV-1 PICs if a second defective IN protomer is present. Yet, when they are the sole IN, the PICs lacked detectable levels of in vitro activity (11, 36) (Fig. 5D), failed to develop mature intasomes (11), and, more often than not, failed to support wild-type levels of reverse transcription (38, 39) (Fig. 2B). Given efficient transcomplementation of active site mutant reporter viruses, the active site mutant protomer is likely to supply an auxiliary function(s) that is essential for proper PIC maturation and/or trafficking. Because HIV-1 IN interacts with a variety of human cell proteins (44), we and others previously proposed that the inability to interact with cell components may be the root cause of the phenotype (17, 38). Alternatively, higher-order interactions specific to formation of the HIV-1 intasome (11) that are independent of cellular components could also be at play. Pinpointing the type(s) of IN-mediated interaction(s) that is likely missing from these types of replication-defective viruses would be expected to define novel targets for antiviral intervention in the fight against HIV/AIDS.

We thank H. Göttlinger and J. Kappes for their generous contributions of reagents.

This work was supported by NIH grants AI39394, AI52014 (A.E.), and AI60354 (Harvard Medical School Center for AIDS Research).

REFERENCES

- Bouyac-Bertoia, M., J. D. Dvorin, R. A. M. Fouchier, Y. Jenkins, B. E. Meyer, L. I. Wu, M. Emerman, and M. H. Malim. 2001. HIV-1 infection requires a functional integrase NLS. *Mol. Cell* 7:1025–1035.
- Broun, A., D. D. Richman, and R. S. Kornbluth. 2001. HIV-1 preintegration complexes preferentially integrate into longer target DNA molecules in solution as detected by a sensitive, polymerase chain reaction-based integration assay. *J. Biol. Chem.* 276:46946–46952.
- Brown, H. E. V., H. Chen, and A. Engelman. 1999. Structure-based mutagenesis of the human immunodeficiency virus type 1 DNA attachment site: effects on integration and cDNA synthesis. *J. Virol.* 73:9011–9020.
- Brown, P. O., B. Bowerman, H. E. Varmus, and J. M. Bishop. 1987. Correct integration of retroviral DNA in vitro. *Cell* 49:347–356.
- Brown, P. O., B. Bowerman, H. E. Varmus, and J. M. Bishop. 1989. Retroviral integration: structure of the initial covalent product and its precursor, and a role for the viral IN protein. *Proc. Natl. Acad. Sci. USA* 86:2525–2529.
- Burke, C. J., G. Sanyal, M. W. Bruner, J. A. Ryan, R. L. LaFemina, H. L. Robbins, A. S. Zeff, C. R. Middaugh, and M. G. Cordingley. 1992. Structural implications of spectroscopic characterization of a putative zinc finger peptide from HIV-1 integrase. *J. Biol. Chem.* 267:9639–9644.
- Bushman, F. D., and R. Craigie. 1991. Activities of human immunodeficiency virus (HIV) integration protein in vitro: specific cleavage and integration of HIV DNA. *Proc. Natl. Acad. Sci. USA* 88:1339–1343.
- Bushman, F. D., A. Engelman, I. Palmer, P. Wingfield, and R. Craigie. 1993. Domains of the integrase protein of human immunodeficiency virus type 1 responsible for polynucleotidyl transfer and zinc binding. *Proc. Natl. Acad. Sci. USA* 90:3428–3432.
- Cai, M., R. Zheng, M. Caffrey, R. Craigie, G. M. Clore, and A. M. Gronenborn. 1997. Solution structure of the N-terminal zinc binding domain of HIV-1 integrase. *Nat. Struct. Biol.* 4:567–577.
- Chen, H., and A. Engelman. 2001. Asymmetric processing of human immunodeficiency virus type 1 cDNA in vivo: implications for functional end coupling during the chemical steps of DNA transposition. *Mol. Cell. Biol.* 21:6758–6767.
- Chen, H., S.-Q. Wei, and A. Engelman. 1999. Multiple integrase functions are required to form the native structure of the human immunodeficiency virus type 1 intasome. *J. Biol. Chem.* 274:17358–17364.
- Chen, J. C.-H., J. Krucinski, L. J. W. Miercke, J. S. Finer-Moore, A. H. Tang, A. D. Leavitt, and R. M. Stroud. 2000. Crystal structure of the HIV-1 integrase catalytic core and C-terminal domains: a model for viral DNA binding. *Proc. Natl. Acad. Sci. USA* 97:8233–8238.
- Chen, Z., Y. Yan, S. Munshi, Y. Li, J. Zugay-Murphy, B. Xu, M. Witmer, P. Felock, A. Wolfe, V. Sardana, E. A. Emini, D. Hazuda, and L. C. Kuo. 2000. X-ray structure of simian immunodeficiency virus integrase containing the core and C-terminal domain (residues 50–293)—an initial glance of the viral DNA binding platform. *J. Mol. Biol.* 296:521–533.
- Craigie, R. 2002. Retroviral DNA integration, p. 613–630. *In* N. L. Craig, R. Craigie, M. Gellert, and A. M. Lambowitz (ed.), *Mobile DNA II*. ASM Press, Washington, DC.
- Craigie, R., T. Fujiwara, and F. Bushman. 1990. The IN protein of Moloney murine leukemia virus processes the viral DNA ends and accomplishes their integration in vitro. *Cell* 62:829–837.
- Dorfman, T., J. Luban, S. P. Goff, W. A. Haseltine, and H. G. Göttlinger. 1993. Mapping of functionally important residues of a cysteine-histidine box in the human immunodeficiency virus type 1 nucleocapsid protein. *J. Virol.* 67:6159–6169.
- Dvorin, J. D., P. Bell, G. G. Maul, M. Yamashita, M. Emerman, and M. H. Malim. 2002. Reassessment of the roles of integrase and the central DNA flap in human immunodeficiency virus type 1 nuclear import. *J. Virol.* 76:12087–12096.
- Eijkelenboom, A. P., F. M. van den Ent, A. Vos, J. F. Doreleijers, K. Hard, T. D. Tullius, R. H. Plasterk, R. Kaptein, and R. Boelens. 1997. The solution structure of the amino-terminal HHCC domain of HIV-2 integrase: a three-helix bundle stabilized by zinc. *Curr. Biol.* 7:739–746.
- Ellison, V., H. Abrams, T. Roe, J. Lifson, and P. Brown. 1990. Human immunodeficiency virus integration in a cell-free system. *J. Virol.* 64:2711–2715.
- Engelman, A. 1999. In vivo analysis of retroviral integrase structure and function. *Adv. Virus Res.* 52:411–426.
- Engelman, A., F. D. Bushman, and R. Craigie. 1993. Identification of discrete functional domains of HIV-1 integrase and their organization within an active multimeric complex. *EMBO J.* 12:3269–3275.
- Engelman, A., and R. Craigie. 1992. Identification of conserved amino acid residues critical for human immunodeficiency virus type 1 integrase function in vitro. *J. Virol.* 66:6361–6369.
- Engelman, A., G. Englund, J. M. Orenstein, M. A. Martin, and R. Craigie. 1995. Multiple effects of mutations in human immunodeficiency virus type 1 integrase on viral replication. *J. Virol.* 69:2729–2736.
- Farnet, C. M., and W. A. Haseltine. 1990. Integration of human immunodeficiency virus type 1 DNA in vitro. *Proc. Natl. Acad. Sci. USA* 87:4164–4168.
- Fletcher, T. M., III, M. A. Soares, S. McPhearson, H. Hui, M. Wiskerchen, M. A. Muesing, G. M. Shaw, A. D. Leavitt, J. D. Boeke, and B. H. Hahn. 1997. Complementation of integrase function in HIV-1 virions. *EMBO J.* 16:5123–5138.
- Fujiwara, T., and K. Mizuuchi. 1988. Retroviral DNA integration: structure of an integration intermediate. *Cell* 54:497–504.
- Hansen, M. S., G. J. R. Smith, T. Kafri, V. Molteni, J. S. Siegel, and F. D. Bushman. 1999. Integration complexes derived from HIV vectors for rapid assays in vitro. *Nat. Biotechnol.* 17:578–582.

28. **Hazuda, D. J., P. Felock, M. Witmer, A. Wolfe, K. Stillmock, J. A. Grobler, A. Espeseth, L. Gabryelski, W. Schleif, C. Blau, and M. D. Miller.** 2000. Inhibitors of strand transfer that prevent integration and inhibit HIV-1 replication in cells. *Science* **287**:646–650.
29. **Jonsson, C., G. Donzella, E. Gaucan, C. Smith, and M. Roth.** 1996. Functional domains of Moloney murine leukemia virus integrase defined by mutation and complementation analysis. *J. Virol.* **70**:4585–4597.
30. **Katz, R. A., G. Merkel, J. Kulkosky, J. Leis, and A. M. Skalka.** 1990. The avian retroviral IN protein is both necessary and sufficient for integrative recombination in vitro. *Cell* **63**:87–95.
31. **Kuiken C., B. Foley, E. Freed, B. Hahn, P. Marx, F. McCutchan, J. Mellors, S. Wolinsky, and B. Korber (ed.).** 2002. HIV sequence compendium 2002, LA-UR number 03–3564. Theoretical Biology and Biophysics Group, Los Alamos National Laboratory, Los Alamos, N. Mex.
32. **Leavitt, A. D., G. Robles, N. Alesandro, and H. E. Varmus.** 1996. Human immunodeficiency virus type 1 integrase mutants retain in vitro integrase activity yet fail to integrate viral DNA efficiently during infection. *J. Virol.* **70**:721–728.
33. **Leavitt, A. D., L. Shiue, and H. E. Varmus.** 1993. Site-directed mutagenesis of HIV-1 integrase demonstrates differential effects on integrase functions in vitro. *J. Biol. Chem.* **268**:2113–2119.
34. **Lee, S. P., J. Xiao, J. R. Knutson, M. S. Lewis, and M. K. Han.** 1997. Zn^{2+} promotes the self-association of human immunodeficiency virus type-1 integrase in vitro. *Biochemistry* **36**:173–180.
35. **Li, L., J. M. Olvera, K. E. Yoder, R. S. Mitchell, S. L. Butler, M. Lieber, S. L. Martin, and F. D. Bushman.** 2001. Role of the non-homologous DNA end joining pathway in the early steps of retroviral infection. *EMBO J.* **20**:3272–3281.
36. **Limón, A., E. Devroe, R. Lu, H. Z. Ghory, P. A. Silver, and A. Engelman.** 2002. Nuclear localization of human immunodeficiency virus type 1 preintegration complexes (PICs): V165A and R166A are pleiotropic integrase mutants primarily defective for integration, not PIC nuclear import. *J. Virol.* **76**:10598–10607.
37. **Lu, R., H. Z. Ghory, and A. Engelman.** 2005. Genetic analyses of conserved residues in the carboxyl-terminal domain of human immunodeficiency virus type 1 integrase. *J. Virol.* **79**:10356–10368.
38. **Lu, R., A. Limón, E. Devroe, P. A. Silver, P. Cherepanov, and A. Engelman.** 2004. Class II integrase mutants with changes in putative nuclear localization signals are primarily blocked at a postnuclear entry step of human immunodeficiency virus type 1 replication. *J. Virol.* **78**:12735–12746.
39. **Lu, R., A. Limón, H. Z. Ghory, and A. Engelman.** 2005. Genetic analyses of DNA-binding mutants in the catalytic core domain of human immunodeficiency virus type 1 integrase. *J. Virol.* **79**:2493–2505.
40. **Nakajima, N., R. Lu, and A. Engelman.** 2001. Human immunodeficiency virus type 1 replication in the absence of integrase-mediated DNA recombination: definition of permissive and nonpermissive T-cell lines. *J. Virol.* **75**:7944–7955.
41. **Pahl, A., and R. M. Flugel.** 1995. Characterization of the human spuma retrovirus integrase by site-directed mutagenesis, by complementation analysis, and by swapping the zinc finger domain of HIV-1. *J. Biol. Chem.* **270**:2957–2966.
42. **Pahl, A., and R. M. Flugel.** 1993. Endonucleolytic cleavages and DNA-joining activities of the integration protein of human foamy virus. *J. Virol.* **67**:5426–5434.
43. **Priet, S., J.-M. Navarro, G. Querat, and J. Sire.** 2003. Reversion of the lethal phenotype of an HIV-1 integrase mutant virus by overexpression of the same integrase mutant protein. *J. Biol. Chem.* **278**:20724–20730.
44. **Turlure, F., E. Devroe, P. A. Silver, and A. Engelman.** 2004. Human cell proteins and human immunodeficiency virus DNA integration. *Front. Biosci.* **9**:3187–3208.
45. **van Gent, D. C., C. Vink, A. A. M. O. Groeneger, and R. H. A. Plasterk.** 1993. Complementation between HIV integrase proteins mutated in different domains. *EMBO J.* **12**:3261–3267.
46. **Wang, J.-Y., H. Ling, W. Yang, and R. Craigie.** 2001. Structure of a two-domain fragment of HIV-1 integrase: implications for domain organization in the intact protein. *EMBO J.* **20**:7333–7343.
47. **Wu, X., H. Liu, H. Xiao, J. A. Conway, E. Hunter, and J. C. Kappes.** 1997. Functional RT and IN incorporated into HIV-1 particles independently of the Gag/Pol precursor protein. *EMBO J.* **16**:5113–5122.
48. **Yang, Z.-N., T. C. Mueser, F. D. Bushman, and C. C. Hyde.** 2000. Crystal structure of an active two-domain derivative of Rous sarcoma virus integrase. *J. Mol. Biol.* **296**:535–548.
49. **Zheng, R., T. M. Jenkins, and R. Craigie.** 1996. Zinc folds the N-terminal domain of HIV-1 integrase, promotes multimerization, and enhances catalytic activity. *Proc. Natl. Acad. Sci. USA* **93**:13659–13664.